Article

Application of Biochar to the Remediation of Pb-Contaminated Solutions

Maria Rosaria Boni, Agostina Chiavola and Simone Marzeddu *

Faculty of Civil and Industrial Engineering, Department of Civil, Constructional and Environmental Engineering (DICEA), Sapienza University of Rome, Via Eudossiana 18, 00184 Rome, Italy; mariarosaria.boni@uniroma1.it (M.R.B.); agostina.chiavola@uniroma1.it (A.C.)
* Correspondence: simone.marzeddu@uniroma1.it; Tel.: +39-06-44585514

check for updates

Abstract: BIOTON® biochar, produced by a wood biomass pyrolysis process, which is usually applied as soil amendment, was investigated for a novel application, i.e., the adsorption of lead from contaminated solutions. The experimental activity included physical and chemical characterization of BIOTON®; and Scanning Electron Microscope (SEM) images to highlight its internal structure. The adsorption process was investigated through batch and column experiments. Adsorption kinetics showed very rapid achievement of equilibrium conditions, i.e., 50 mg/L and 100 mg/L initial Pb concentration at 2 h and 4 h, respectively. Complete removal also occurred within the same time. The Brunauer–Emmett–Teller model was a better fit for the equilibrium data of both Pb concentrations, whereas the kinetics were best represented by the pseudo second-order model. Column tests showed that the addition of biochar as an adsorbent media within the bed significantly extended the time of breakthrough and exhaustion, with respect to the column filled with soil only. The values found for the adsorption capacity of BIOTON®- versus lead-containing solutions were comparable to those reported for commercial adsorbents. Therefore, BIOTON® can be considered a valid option: It also offers the additional benefit of allowing the recovery of a residue, which alternately would need to be disposed of.

Keywords: adsorption; batch; biochar; column; lead; remediation

1. Introduction

Biochar obtained from the pyrolysis of woody biomass can be used for a number of purposes, such as for soil amendment [1–4], and as a low cost adsorbent [5–10]. As far as the former application is concerned, biochar has been demonstrated to improve soil properties [11–17], as well as to reduce contaminant leaching [18–23]. As an adsorbent, it represents a more economically and environmentally sustainable alternative to commercial media. This is due to the fact that its use allows for avoiding industrial activities related to adsorbent production, and its reuse allows for avoiding a waste that alternatively would need to be disposed of.

Biochar can be applied as an adsorbent to water and wastewater treatment for a wide range of pollutants such as lead, arsenic, copper, cadmium, chromium, mercury, zinc, and nickel [10,24–26].

Lead is among a list of dangerous substances as indicated by the Agency for Toxic Substances and Disease Registry (ATSDR) [27]. Due to the associated risks, Italian legislation requires Pb concentration to be below 10 µg/L in groundwater (Italian decree n. 152/06), and 0.2 mg/L in the streams released into surface waters [28].

High levels of heavy metals, and particularly of Pb, in soil and water have been reported worldwide [29–31]. Sources of contamination can be different: E.g., improper operation of industrial

processes, and deposition on soil of old lead-containing fuels. Due to its harmful consequences on human health, it is mandatory to avoid entry of lead-contaminated waters into the food chain [32].

Several technologies have been developed to intercept lead and prevent it from spreading into the environment. For instance, there are some substances, such as biochar, which can be applied to contaminated soils to reduce metal mobilization. Indeed, heavy metals become bound to carbonates and organic matter after biochar incorporation: The consequence is the enhancement of the adsorption process due to metals building bonds with oxygen-, carbon-, and nitrogen-containing functional groups [21,33,34]. In addition, the high pH, Cation Exchange Capacity (CEC), microporous structure, and excess of soluble salts on the biochar surface increase the heavy metal immobilization through precipitation and surface adsorption [21,35,36].

Biochar is a substance that derives from the pyrolysis of selected plant biomasses [37,38]. Currently, it is mainly used as a soil improver; however, its adsorbent properties suggest it could also be used for metal sequestering, thus reducing mobility and danger. For instance, it has been demonstrated that by applying biochar to soil, pH can be effectively modified and metal solubilization prevented [39–41].

Biochar has been also investigated as an adsorbent for remediating water contaminated by heavy metals [5,7,10,42–47]. The quality and properties of biochar depend on many factors [23]; it is essential to identify the characteristics of this adsorbent to predict its effectiveness towards the target contaminant.

Many biochars have a high adsorption capacity for metal contaminants because of their high heterogeneous specific surface [48], and their well-distributed pore network that includes micropores (<2 nm), mesopores (2–50 nm), and macropores (>50 nm) [49].

In the present study, a biochar produced in Italy as a soil improver was investigated for a different application, i.e., adsorption of lead from aqueous solutions. Kinetics and uptake capacity were evaluated through batch tests using two contaminated solutions, at 50 and 100 mg/L Pb. Furthermore, column tests were conducted, and breakthrough curves determined using lab-scale plants filled with the same biochar and fed by a solution at 100 mg/L Pb.

It is noteworthy that this was the first application of the examined biochar as an adsorbent for lead removal from aqueous solution, particularly in a column plant.

2. Materials and Methods

2.1. Biochar

BIOTON®, supplied by the LATERIZI REATO S.r.l., was used in the present experimentation; it was produced by a wood biomass pyrolysis process, at a temperature below 750 °C, in a controlled atmosphere with low oxygen content. Due to processing issues, semi-decorticated and large-sized wood was used, in particular poplar, oak, robinia, platanus, willow, apple, and pear wood; resinous wood like fir, larch, pine or conifers was not used. The biochar had a capacity of imbibition above 250% by volume, a specific weight ranging from 0.125 to 0.150, which was evaluated on the anhydrous product after the production process at humidity less than 7%.

The Company who provided the biochar developed the technology for extracting syngas from biomass: This consisted of an open-core downdraft pyrolyzer with a continuous feeding equicurrent, without a water scrubber, and with a high temperature filtration and separation system.

2.2. Analytical Methods

Lead concentrations were determined using a Perkin Elmer atomic absorption spectrophotometer with flame atomization (F-AAS; Perkin-Elmer model 3030B), whose detection limit was 0.1 mg/L. The calibration curve was determined using standard solutions at 2 mg/L and 4 mg/L Pb [50].

The biochar was chemically and physically characterized using the procedures described in the literature [51–53]. Particularly, the following parameters were determined on representative samples of biochar: Bulk density, field capacity, porosity, moisture content, ash content, pH, and pH point of

zero charge. Biochar samples were also analyzed using a HR FESEM Zeiss Auriga (SEM; Rome, Italy) at 3000× magnification and 10 kV acceleration voltage, to provide the elemental analysis of the surface (EDX) and to obtain a qualitative indication of the major components.

2.3. Chemical Solutions

Lead solutions were prepared by adding a known amount of lead nitrate salt (supplied by Carlo Erba, Milan, Italy) into ultrapure water in order to obtain final concentrations of 50 and 100 mg/L.

All reagents were of analytical grade and were used without any further purification.

2.4. Batch Tests

Batch experiments were carried out using the jar-tester apparatus to determine the kinetic characteristics and the isotherms of the adsorption process of lead onto the BIOTON® biochar. The experiments were conducted at 50 and 100 mg/L of lead as initial concentrations. These values were selected for being very high and far above the limits posed by the Italian legislation (10 µg/L for groundwater, and 0.2 mg/L for release into surface waters), in order to test the adsorption capacity of the media under severe conditions, similar to what has been reported by other studies [44]. In the batch tests, 1.25 of biochar was added to 250 mL of a Pb-contaminated solution, and this was maintained under mixing conditions for 6 h, at 120 rpm constant stirring speed. Samples were then taken at different times: Particularly at 5, 15, 30, 45, and 60 min within the first hour, and afterwards at 1 h intervals until the end of the tests.

Through the above batch tests, it was possible to determine the equilibrium time of the adsorption process. The kinetics data were analyzed using the following models: Zero, first, second, saturation, pseudo-first, and pseudo-second-order. The best fitting model between the experimental and the modeled data was determined based on the value of the regression coefficient, R^2.

Further batch tests were conducted with the aim of obtaining the isotherms. To this end, different adsorbent dosages of BIOTON® were added to 250 mL solutions (at 50 and 100 mg/L Pb concentrations), and these solutions were maintained under mixing conditions for a duration equal to the equilibrium time previously determined.

At the end of the tests, liquid samples were collected and analyzed for the residual Pb concentration in the solution. The equilibrium data were fitted by the Langmuir, Freundlich, and Brunauer–Emmett–Teller (BET) isotherm models [54–56]. The best fitting model was determined based on the value of R^2.

Lead percentage removal (R%), lead adsorbed per unit weight of adsorbent at time t (q_t), and at the equilibrium time (q_e), were calculated using the following Equations (1), (2), and (3), respectively), obtained through the mass balance of lead between the liquid and solid phases [57]:

$$R\% = \frac{(C_0 - C_t)}{C_0} \, 100\% \tag{1}$$

$$q_t = \frac{(C_0 - C_t)V}{m} \tag{2}$$

$$q_e = \frac{(C_0 - C_e)V}{m} \tag{3}$$

where V is the volume of the aqueous solution, m is the mass of BIOTON®, C_0 (equal to 50 and 100 mg/L Pb, respectively), C_t and C_e indicate lead concentration in the liquid phase at time t = 0, t and at equilibrium, respectively. Batch experiments were conducted in duplicate and the results obtained were averaged.

2.5. Column Tests

Biochar characteristics as an adsorbent medium in a column plant were investigated using a lab-scale apparatus. These tests were performed following the procedures outlined in a previous paper by the same authors [58].

Laboratory columns were 18 cm high and 1 cm in diameter.

The columns were filled by alternating layers of sand, biochar, and soil. Particularly, a previously sterilized quartz sand was placed on the bottom; a layer of BIOTON® (mass of 0.5 g) was posed above; followed on the top by 1 g of agricultural soil (made by 29% clay, 28% silt, 43% sand, and 2% organic matter, by weight).

Particle sizes smaller than 2 mm were chosen for biochar and sand, in order to limit by-pass phenomena along the column walls [59,60]. One more column, filled with soil only, was operated under the same conditions as a control.

The lead contaminated solution, at a concentration C_0 = 100 mg/L Pb, was continuously fed to the top of the columns through peristaltic pumps, at 60 mL/h flow rate. This high concentration of lead was chosen to test the biochars adsorbent characteristics under severe conditions, and to obtain a rapid development of the breakthrough curve.

Eluates were collected from the bottom of the columns at prefixed times, and analyzed for their residual Pb concentration. Breakthrough curves were determined by recording Pb concentrations in the eluates versus cumulative solution volumes fed to the columns. These curves determined the breakpoint and saturation times, which represented the time when the Pb concentration in the eluate, C, started to rise above 0 and when it reached the value in the influent, i.e., C_0, respectively. The experimental data of the column tests were fitted using the Yoon–Nelson [61], Thomas [62], and Bohart–Adams [63] models [64,65].

3. Results

3.1. Biochar Characterization

Initial characterization of BIOTON® provided the values of its main physical and chemical properties, which are listed in Table 1. This table shows the type of property, the unit, and the method or instrument used for the determination. Particularly, reported in brackets are the references to the analytical method or type of analytical equipment used for the characterization.

Table 1. Main physical and chemical properties of BIOTON® (% on dry weight).

Physical and Chemical Properties	Symbol	Unit	Values	Methods and Instruments
Bulk density	γ_s	g/cm^3	1.98	[51,52]
Specific weight	γ_d	g/cm^3	0.235	[51,52]
Field capacity	ω_c	g in 100 g	650	[51,52]
Porosity	N	%	88.14	[51,52]
Carbon	C	%	89.25	Zeiss Auriga
Oxygen	O	%	7.46	Zeiss Auriga
Potassium	K	%	1.22	Zeiss Auriga
Calcium	Ca	%	1.01	Zeiss Auriga
Magnesium	Mg		0.37	Zeiss Auriga
Silicon	Si		0.26	Zeiss Auriga
Sodium	Na		0.20	Zeiss Auriga
Moisture content	ω	%	29.11	[51,52]
Ash content	cc	%	60.91	[51,52]
Potential of Hydrogen	pH	-	10.4	[51,52]
Point of zero charge	pH_{PZC}	-	10.5	[66]

Values in Table 1 of elemental analysis were obtained by the technical sheet of biochar, while other parameters were determined experimentally. The Scanning Electron Microscope (SEM) images of

BIOTON® surface are shown in Figure 1, at various magnifications: (A) 79 X; (B) 2.50 KX; (C) 2.00 KX; and (D) 100.00 KX.
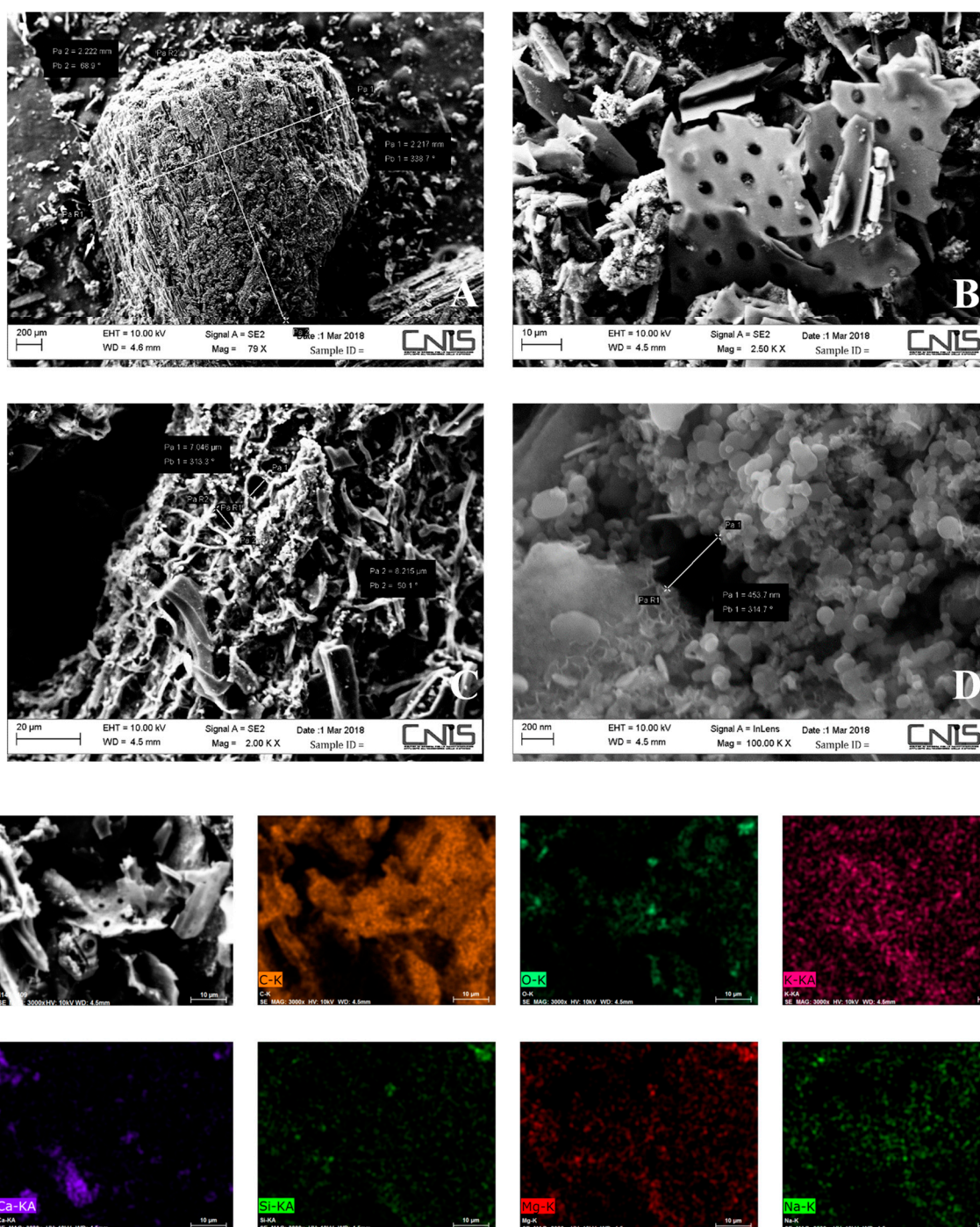

Figure 1. Scanning Electron Microscope (SEM) images of the surface, and image and color coded Energy Dispersive X-ray (EDX) analysis dot maps of BIOTON®, at different magnifications: (**A**) 79 X; (**B**) 2.50 KX; (**C**) 2.00 KX; and (**D**) 100.00 KX.

Particularly, in Figure 1; (A) highlighted the particle size, (B) the different feedstocks used for biochar production, (C) the cross-section, and (D) the internal pores. Figure 1 shows also the elemental maps of carbon, oxygen, potassium, calcium, silicon, magnesium, and sodium within the biochar samples, whose percentage content is reported in Table 1: Amber color was used to indicate carbon,

aquamarine for oxygen, magenta for potassium, dark violet for calcium, green yellow for silicon, red for magnesium, and green for sodium.

3.2. Batch Tests

Figure 2 shows lead percentage removal versus time, in the batch tests conducted at concentrations of 50 mg/L and 100 mg/L Pb. It can be observed that the removal rate was very rapid in the first 30 min in the case of 50 mg/L, and reached almost 100% by the first hour of the test. In the case of 100 mg/L, the slope was still very rapid in the first 30 min, although afterwards it proceeded more slowly reaching R = 100% in about 4 h. The linearized form of the equation of different kinetic models was used to find out which was best fitting of the experimental data. The pseudo second-order model provided the best agreement between the modeled and the experimental data, as highlighted by the highest value of the correlation coefficient, R^2. Figure 3 shows the experimental and the modeled data in terms of t/q_t versus t. Through the slope and intercept of the regression line, it was possible to determine the values of the pseudo second-order rate constant, k_s, and of the amount of Pb adsorbed at equilibrium per unit weight of BIOTON®, q_e, which are reported in Table 2. The same table also contains the value of $q_{e,exp}$ which represented the value of q that was experimentally calculated at t = 300 min, which was assumed to be the equilibrium time. It can be noted that the experimental and the modeled data did not differ appreciably at both 50 mg/L and 100 mg/L Pb.

Table 2. Pseudo second-order kinetic model and adsorption Brunauer–Emmett–Teller (BET) isotherm parameters.

	Pseudo Second-Order Kinetic Model				BET Isotherm		
C_0 (mg/L)	$q_{e,exp}$ (mg/g)	q_e (mg/g)	k_s (g/min)	R^2 -	q_{max} (mg/g)	C_{BET} (L/mg)	R^2 -
50	9.95	9.74	0.0049	0.9730	22.00	2,530,403.46	0.6952
100	20.30	20.08	0.0141	0.9993	168.98	373,280.22	0.9981

Equilibrium data were best fitted by the BET isotherm model for both contaminated solutions at 50 mg/L and 100 mg/L (higher R^2). Table 2 shows the values of the BET parameters, i.e., C_{BET} which was a constant linked to the energy of interaction between solute and adsorbent, C_s, represented the solute saturation concentration, and q_{max} which indicated the amount of adsorbate per unit mass of adsorbent at equilibrium, corresponding to a complete monomolecular layer of adsorbate formed on the surface of the adsorbent. Figure 4 shows the plots of $C_e/q_e(C_s-C_e)$ versus C_e/C_s, at both Pb concentrations.
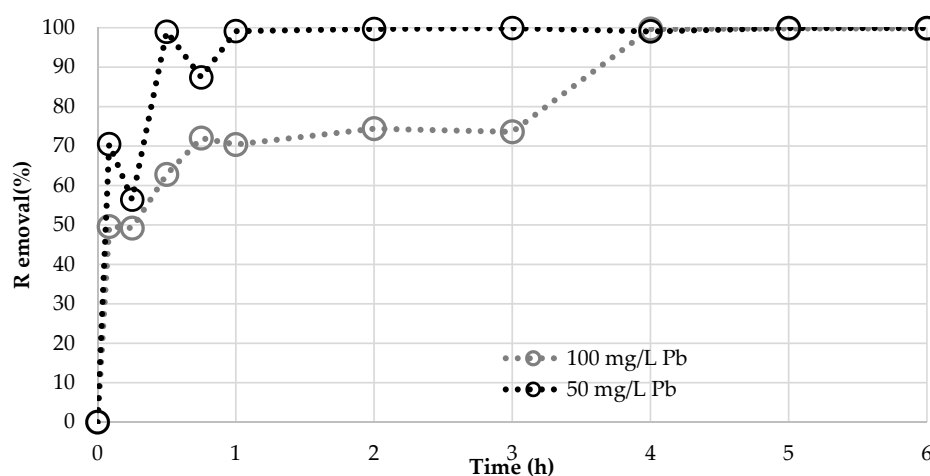

Figure 2. Lead percentage removal versus contact time. Adsorption temperature, mixing rate, and dosage were maintained at 20 ± 0.5 °C, 120 RPM, and 5 g/L, respectively.
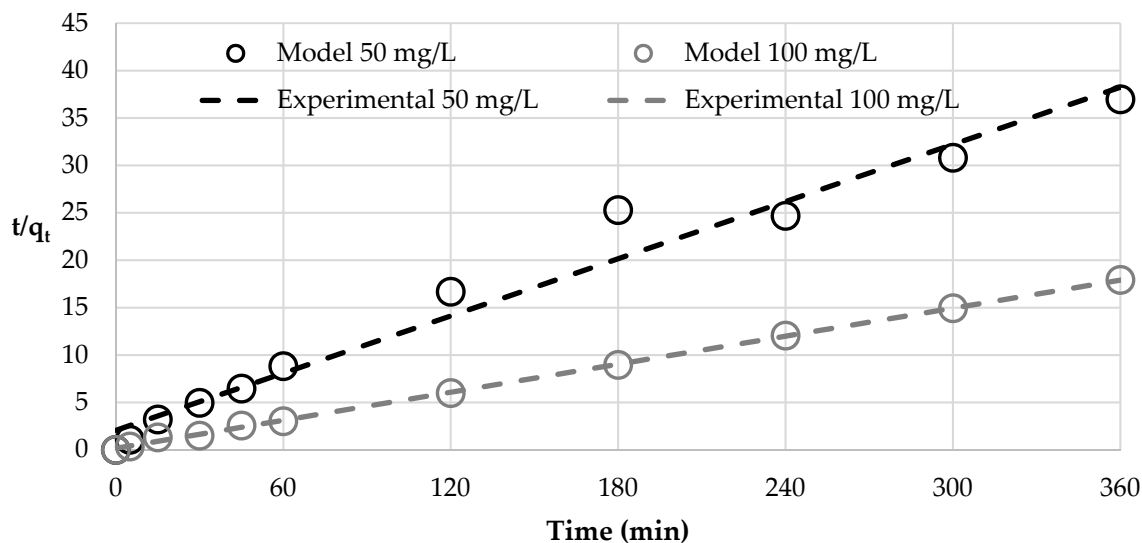
Figure 3. Experimental data and modeling by the linearized pseudo second-order kinetic equation. Adsorption temperature, mixing rate, and dosage were maintained at $20 \pm 0.5\ °C$, 120 RPM, and 5 g/L, respectively.
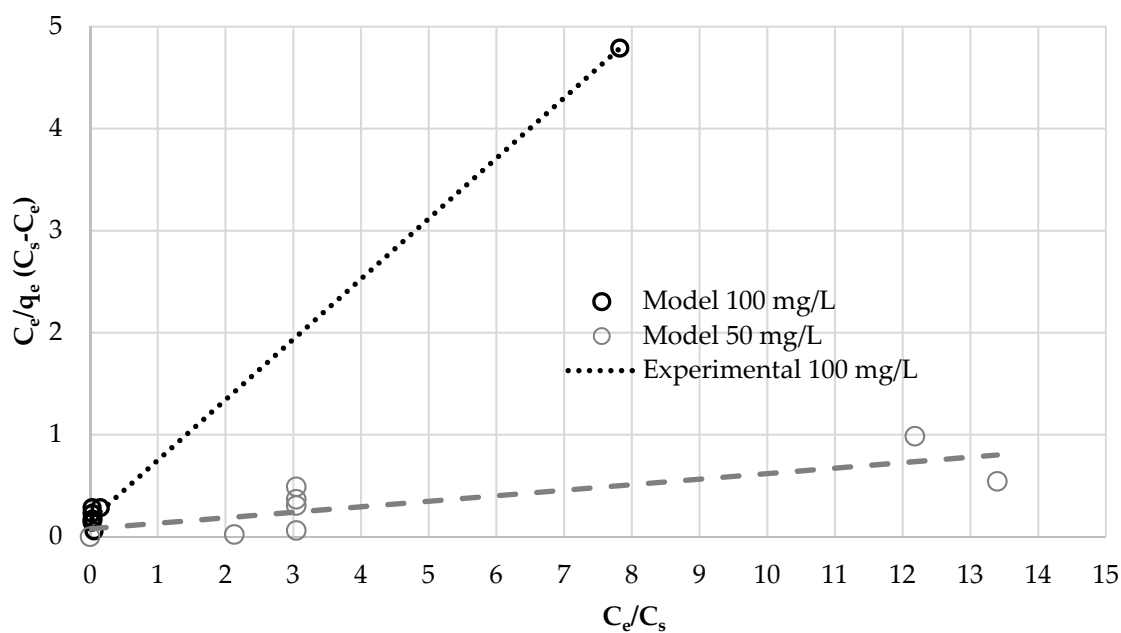

Figure 4. Isotherm experimental data and modeling by the linearized BET equation. Adsorption temperature, mixing rate, and equilibrium time were maintained at $20 \pm 0.5\ °C$, 120 RPM, and 5 h, respectively.

The ability of BIOTON$^®$ to remove lead as a function of the adsorbent mass is shown in Figure 5, in terms of removal percentage versus adsorbent dosage.

Figure 5 shows that the removal percentage increased rapidly by rising the dosage: R% = 100% was reached for 0.5 g/L and 1 g/L BIOTON$^®$, at 50 mg/L and 100 mg/L Pb concentrations, respectively. Above this dosage, further increases did not determine any appreciable improvement of R%.
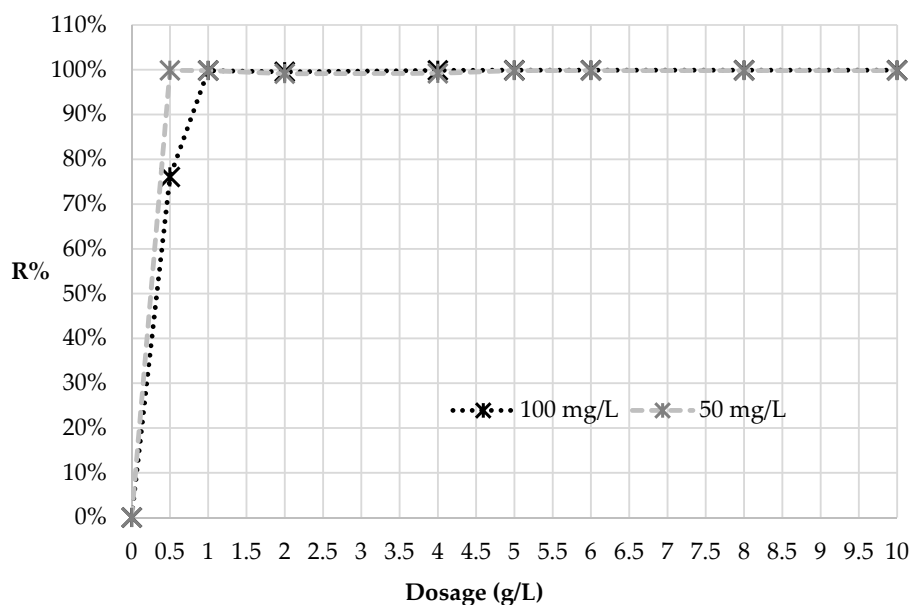
Figure 5. Percentage of lead removal in both contaminated solutions versus different BIOTON® dosages. Adsorption temperature, mixing rate, and equilibrium time were maintained at 20 ± 0.5 °C, 120 RPM, and 5 h, respectively.

3.3. Column Tests

Figure 6 shows the breakthrough curves obtained through the column tests. They were plotted in terms of the percentage of Pb concentration in the eluate with respect to the feeding concentration, C/C_0, versus time of operation of the column plant filled with soil only, and soil with BIOTON®, respectively.
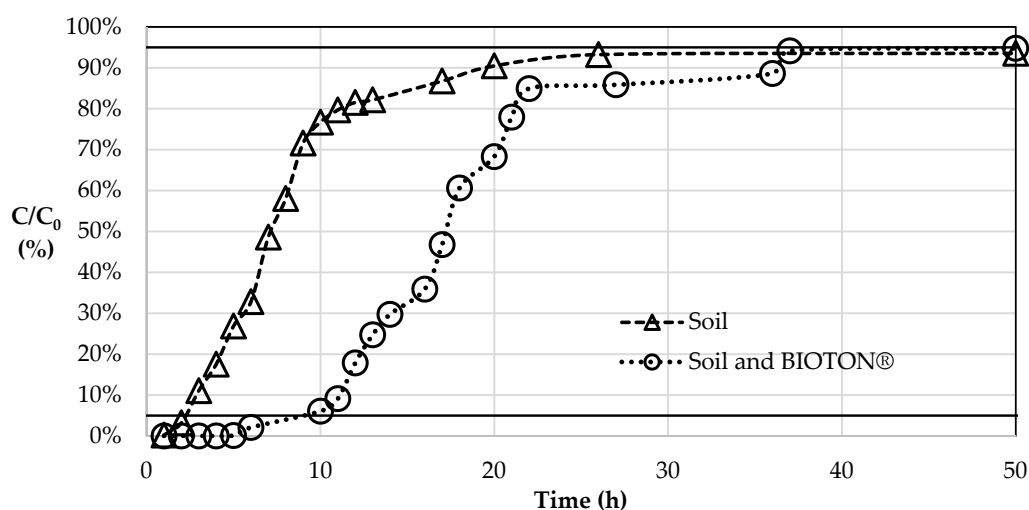

Figure 6. Breakthrough curves for adsorption of Pb onto soil and soil with BIOTON®. Adsorption temperature, flow rate, and initial concentration were maintained at 20 ± 0.5 °C, 60 mL/h, and 100 mg/L, respectively.

Figure 6 shows also two horizontal lines drawn at $C/C_0 = 5\%$ and $C/C_0 = 95\%$, assumed to represent breakthrough and the exhaustion conditions, respectively.

The breakthrough curves obtained for soil and soil with biochar had approximately the same shape: A rapid increase of C/C_0 after breakthrough, followed by a trend at a much slower rate towards the exhaustion.

By integrating the breakthrough curve between t = 0 and t = 50 h (end of the column tests), it was possible to determine the experimental value of the adsorption capacity, which was q_{exp} = 177.80 mg/g for the column filled with soil and BIOTON®. This value takes into account the capacity of both media, which contributed for 67.07 mg/g and 110.73 mg/g for soil and BIOTON®, respectively.

Among the three mathematical models applied, the Thomas model provided a better description of the experimental breakthrough curves [62] (R^2 = 0.76), when compared to Yoon–Nelson (R^2 = 0.60) [61], and Bohart–Adams (R^2 = 0.61) [63]. The Thomas rate constant (k_{TH}) and the adsorption capacity (q_0) were obtained from the linearized form of the model equation, by plotting $\ln(C_0/C\text{-}1)$ versus t (not here shown), and by determining the intercept and the slope of the regression line. The values found were: k_{TH} = 4.10 × 10^{-5} mL/min·mg and q_0 = 270.57 mg/g.

4. Discussion

With respect to Table 1 showing chemical and physical properties of the investigated biochar, values of carbon and oxygen contents were similar to those reported by [14,53], for the products of pyrolysis of different feedstocks conducted at 700 °C and 600 °C. The ash content, found to be about 60%, was probably due to the high pyrolysis temperature (700 °C). In a recent study, an ash content of about 40% at a pyrolysis temperature of 500 °C was observed [67]. In the same paper, the value reported for pH_{PZC} was equal to that found in the present study, i.e., 10.5.

The removal percentage shown in Figure 2 depicted a common profile at both tested concentrations: A rapid rate occurring in the first hour, which was followed by a much slower phase that reached equilibria in about 2 h and 4 h at 50 mg/L and 100 mg/L, respectively. Negligible variations were observed afterwards. In Figure 2, the first removal phase could be attributed to a rapid occupation of the more easily accessible external surface sorption sites, while the slower phase could be related to the formation of inner layer complexes after saturation of outer sorption sites [68].

The profile observed in the present study was consistent with the scientific literature: In [68], a similar profile was reported of Pb adsorption at the same initial concentration onto biochar from pyrolysis of pig and cow manure at 400 °C and 600 °C, although at a slower rate (equilibria was reached after 5 h). Another study indicated equilibrium times after about 4 h and 30 min for the adsorption of 50 mg/L Pb onto biochar made from a mixture of wood chips, green waste, rice hull, corn cob, nut shells and husks, and cotton gin trash and pomace [69]. Therefore, using different feedstocks for biochar production gives rise to change in the equilibrium time of the adsorption process of lead on this adsorbent.

The pseudo second-order model provided the best agreement for both Pb concentrations (higher R^2 value) with respect to the other models applied [57]. The pseudo second-order equation assumed that the rate of occupation of adsorption sites was proportional to the square of the number of unoccupied activated sites on the surface of the adsorbent [57].

Table 2 shows the values determined of the specific adsorption capacity and of the rate constant of the model. It can be noted that the value of q_e increased more than double, as the Pb concentration rose from 50 mg/L to 100 mg/L.

Regarding the equilibrium data, the BET isotherm model provided the best agreement of the experimental data at both Pb concentrations (higher R^2 value). BET isotherm represented an extension of the Langmuir model to the case of multimolecular adsorption [70]. The model is generally applied to the case of physical adsorption, with the formation of several layers of adsorbate on the surface of the adsorbent [55]. Table 2 highlights the good agreement of the model with the experimental data obtained at 100 mg/L Pb. By contrast, the BET fitting was not as good for the solution at 50 mg/L; however, the BET model still provided a better fitting than Langmuir and Freundlich isotherms (R^2 = 0.4501, and R^2 = 0.2780, respectively). The correlation coefficient was not very high in the case of 50 mg/L Pb likely due to the fact that the removal process was particularly efficient: Indeed, at all the adsorbent dosages, at the end of the tests an equilibrium concentration below the detection level of 0.1 mg/L was achieved. Therefore, it was difficult to obtain a good fitting of the data. This suggested

the opportunity to use lower dosages at this level of contamination, which would allow saving on adsorbent usage.

In terms of implementation at full-scale, adsorbents with the highest value of the maximum adsorption capacity, q_{max}, are the most desirable. The values found in the present study for BIOTON$^®$ fell within the ranges reported by the literature [7,42] for different biochars and Pb removal from water [7,71–76]. In [77], by applying hydrochar produced from peanut hull to an initial Pb concentration of 50 mg/L, it was found that the value of the maximum lead sorption capacity was very similar to that obtained in the present study (i.e., 22.82 mg/g, and 22.00 mg/g, respectively). By contrast, using biochar derived from anaerobically digested sugarcane bagasse at an initial Pb concentration of 100 mg/L, it was found at a lower value, i.e., 135.48 mg/g, with respect to 168.98 mg/g observed in the present work [71]. The differences were likely due to the change in the type and operating conditions of the production process, which have been known to affect the porosity and microstructure of the adsorbents [71,77].

From the results reported in Figure 5, it was possible to assess that for Pb contaminated solutions at 50 mg/L and 100 mg/L, using a dosage of 1 g/L of BIOTON$^®$ as adsorbent would make it possible to comply with the limit set by the Italian legislation for its release into surface waters (equal to 0.2 mg/L). The breakthrough curves of the adsorption of Pb onto soil and soil with BIOTON$^®$, as reported in Figure 6, highlighted that the addition of biochar significantly enhanced the adsorption capacity of the column plant: Indeed, both breakthrough and exhaustion conditions were reached more rapidly in the column filled with soil only with respect to the column also containing biochar (about 2 h versus 10 h).

No reference could be found in the specialized literature on the application of biochar as an adsorbent media, in a column plant, for lead removal from water. Therefore, these data could not be evaluated in comparison with other experimental studies.

Among the models applied for fitting the experimental breakthrough curves, the Thomas model provided the best fitting. The value of the adsorption capacity predicted by this model, i.e., $q_0 = 270.57$ mg/g, was much higher than the value experimentally determined, i.e., $q_{exp} = 177.80$ mg/g: The difference indicated that the media did not reach the exhaustion condition at the end of the tests, i.e., at t = 50 h, and therefore it still possessed adsorption sites to be occupied by the adsorbate. It is worth noting that in continuous flow column plant, a higher adsorption capacity than that measured under batch conditions was expected, due to the higher driving force of the process. Furthermore, the value of q_0 predicted by the model was very similar to the data reported in the specialized literature for the maximum adsorption capacity of Pb by adsorbents other than biochar in column plants [7,71–76].

5. Conclusions

BIOTON$^®$ biochar produced from various wood biomasses through a pyrolysis process showed to be highly efficient as an adsorbent for lead contaminated solutions at 50 mg/L and 100 mg/L.

BET isotherm provided the best agreement between the experimental data of equilibrium, and the BET constants and the maximum adsorption capacity equal to: $C_{BET} = 2,530,403.46$ L/mg and $q_{max} = 22.00$ mg/g at 50 mg/L Pb, and $C_{BET} = 373,280.22$ L/mg and $q_{max} = 168.98$ mg/g at 100 mg/L Pb.

The pseudo second-order model was found to be the best at both concentrations, with $k_s = 0.0049$ g/min and $k_s = 0.141$ g/min.

The column tests showed a significant extension of the breakthrough and exhaustion times in the plant filled with soil and biochar with respect to the plant filled with soil only. The Thomas model provided the best agreement of the experimental breakthrough curves, with the constant $k_{TH} = 4.10 \times 10^{-5}$ mL/min·mg. The maximum adsorption capacity predicted by the model was found to be $q_0 = 270.57$ mg/g, which was similar to the values reported by the specialized literature for commercial adsorbents used in column plants for the treatment of lead contaminated solutions.

These results highlight that the use of BIOTON® as an adsorbent represents a valid option to commercial adsorbents: It offers a good adsorption efficiency, and reduces the amount of vegetable waste to be disposed of, thus contributing to the virtuous cycles of waste recovery and reuse.

Further studies should be conducted to obtain a deeper characterization of BIOTON® properties; besides, its adsorption capacity should be evaluated in the presence of multi-contaminant solutions in view of full-scale applications.

References

1. Xie, T.; Reddy, K.R.; Wang, C.; Yargicoglu, E.; Spokas, K. Characteristics and applications of biochar for environmental remediation: A review. *Crit. Rev. Environ. Sci. Technol.* **2015**, *45*, 939–969. [CrossRef]

2. Agegnehu, G.; Bass, A.M.; Nelson, P.N.; Bird, M.I. Benefits of biochar, compost and biochar-compost for soil quality, maize yield and greenhouse gas emissions in a tropical agricultural soil. *Sci. Total Environ.* **2016**, *543*, 295–306. [CrossRef] [PubMed]

3. Qian, K.; Kumar, A.; Zhang, H.; Bellmer, D.; Huhnke, R. Recent advances in utilization of biochar. *Renew. Sustain. Energy Rev.* **2015**, *42*, 1055–1064. [CrossRef]

4. Lehmann, J.; Joseph, S. Biochar for environmental management: An introduction. *Biochar Environ. Manag. Sci. Technol.* **2009**, *1*, 33–46. [CrossRef]

5. Ahmad, M.; Rajapaksha, A.U.; Lim, J.E.; Zhang, M.; Bolan, N.; Mohan, D.; Vithanage, M.; Lee, S.S.; Ok, Y.S. Biochar as a sorbent for contaminant management in soil and water: A review. *Chemosphere* **2014**, *99*, 19–23. [CrossRef] [PubMed]

6. Cha, J.S.; Park, S.H.; Jung, S.C.; Ryu, C.; Jeon, J.K.; Shin, M.C.; Park, Y.K. Production and utilization of biochar: A review. *J. Ind. Eng. Chem.* **2016**, *40*, 1–15. [CrossRef]

7. Inyang, M.I.; Gao, B.; Yao, Y.; Xue, Y.; Zimmerman, A.; Mosa, A.; Pullammanappallil, P.; Ok, Y.S.; Cao, X. A review of biochar as a low-cost adsorbent for aqueous heavy metal removal. *Crit. Rev. Environ. Sci. Technol.* **2016**, *46*, 406–433. [CrossRef]

8. Gwenzi, W.; Chaukura, N.; Noubactep, C.; Mukome, F.N.D. Biochar-based water treatment systems as a potential low-cost and sustainable technology for clean water provision. *J. Environ. Manag.* **2017**, *197*, 732–749. [CrossRef] [PubMed]

9. Rosales, E.; Meijide, J.; Pazos, M.; Sanromán, M.A. Challenges and recent advances in biochar as low-cost biosorbent: From batch assays to continuous-flow systems. *Bioresour. Technol.* **2017**, *246*, 176–192. [CrossRef] [PubMed]

10. De Gisi, S.; Lofrano, G.; Grassi, M.; Notarnicola, M. Characteristics and adsorption capacities of low-cost sorbents for wastewater treatment: A review. *Sustain. Mater. Technol.* **2016**, *9*, 10–40. [CrossRef]

11. Agegnehu, G.; Srivastava, A.K.; Bird, M.I. The role of biochar and biochar-compost in improving soil quality and crop performance: A review. *Appl. Soil Ecol.* **2017**, *119*, 156–170. [CrossRef]

12. Jien, S.H.; Chen, W.C.; Ok, Y.S.; Awad, Y.M.; Liao, C. Sen Short-term biochar application induced variations in C and N mineralization in a compost-amended tropical soil. *Environ. Sci. Pollut. Res.* **2018**, *25*, 25715–25725. [CrossRef] [PubMed]

13. Luo, S.; Wang, S.; Tian, L.; Li, S.; Li, X.; Shen, Y.; Tian, C. Long-term biochar application influences soil microbial community and its potential roles in semiarid farmland. *Appl. Soil Ecol.* **2017**, *117–118*, 10–15. [CrossRef]

14. Suliman, W.; Harsh, J.B.; Abu-Lail, N.I.; Fortuna, A.M.; Dallmeyer, I.; Garcia-Pérez, M.; Garcia-Perez, M. The role of biochar porosity and surface functionality in augmenting hydrologic properties of a sandy soil. *Sci. Total Environ.* **2017**, *574*, 139–147. [CrossRef] [PubMed]

15. Hagemann, N.; Joseph, S.; Schmidt, H.P.; Kammann, C.I.; Harter, J.; Borch, T.; Young, R.B.; Varga, K.; Taherymoosavi, S.; Elliott, K.W.; et al. Organic coating on biochar explains its nutrient retention and stimulation of soil fertility. *Nat. Commun.* **2017**, *8*, 1089. [CrossRef] [PubMed]

16. Burrell, L.D.; Zehetner, F.; Rampazzo, N.; Wimmer, B.; Soja, G. Long-term effects of biochar on soil physical properties. *Geoderma* **2016**, *282*, 96–102. [CrossRef]

17. Blanco-Canqui, H. Biochar and Soil Physical Properties. *Soil Sci. Soc. Am. J.* **2017**, *84*, 687–711. [CrossRef]

18. Zong, Y.; Wang, Y.; Sheng, Y.; Wu, C.; Lu, S. Ameliorating soil acidity and physical properties of two contrasting texture Ultisols with wastewater sludge biochar. *Environ. Sci. Pollut. Res.* **2018**, *25*, 25726–25733. [CrossRef] [PubMed]

19. Lomaglio, T.; Hattab-Hambli, N.; Miard, F.; Lebrun, M.; Nandillon, R.; Trupiano, D.; Scippa, G.S.; Gauthier, A.; Motelica-Heino, M.; Bourgerie, S.; et al. Cd, Pb, and Zn mobility and (bio)availability in contaminated soils from a former smelting site amended with biochar. *Environ. Sci. Pollut. Res.* **2018**, *25*, 25744–25756. [CrossRef] [PubMed]

20. Haider, G.; Steffens, D.; Moser, G.; Müller, C.; Kammann, C.I. Biochar reduced nitrate leaching and improved soil moisture content without yield improvements in a four-year field study. *Agric. Ecosyst. Environ.* **2017**, *237*, 80–94. [CrossRef]

21. Yin, D.; Wang, X.; Chen, C.; Peng, B.; Tan, C.; Li, H. Varying effect of biochar on Cd, Pb and As mobility in a multi-metal contaminated paddy soil. *Chemosphere* **2016**, *152*, 196–206. [CrossRef] [PubMed]

22. Puga, A.P.; Abreu, C.A.; Melo, L.C.A.; Beesley, L. Biochar application to a contaminated soil reduces the availability and plant uptake of zinc, lead and cadmium. *J. Environ. Manag.* **2015**, *159*, 86–93. [CrossRef] [PubMed]

23. Tang, J.; Zhu, W.; Kookana, R.; Katayama, A. Characteristics of biochar and its application in remediation of contaminated soil. *J. Biosci. Bioeng.* **2013**, *116*, 653–659. [CrossRef] [PubMed]

24. Ifthikar, J.; Wang, T.; Khan, A.; Jawad, A.; Sun, T.; Jiao, X.; Chen, Z.; Wang, J.; Wang, Q.; Wang, H.; et al. Highly Efficient Lead Distribution by Magnetic Sewage Sludge Biochar: Sorption Mechanisms and Bench Applications. *Bioresour. Technol.* **2017**, *238*, 399–406. [CrossRef] [PubMed]

25. Ding, Z.; Hu, X.; Wan, Y.; Wang, S.; Gao, B. Removal of lead, copper, cadmium, zinc, and nickel from aqueous solutions by alkali-modified biochar: Batch and column tests. *J. Ind. Eng. Chem.* **2016**, *33*, 239–245. [CrossRef]

26. Lu, H.; Zhang, W.; Yang, Y.; Huang, X.; Wang, S.; Qiu, R. Relative distribution of Pb2+sorption mechanisms by sludge-derived biochar. *Water Res.* **2012**, *46*, 854–862. [CrossRef] [PubMed]

27. Abadin, H.; Ashizawa, A.; Stevens, Y.-W.; Llados, F.; Diamond, G.; Sage, G.; Citra, M.; Quinones, A.; Bosch, S.J.; Swarts, S.G. *Toxicological Profile for Lead*; US Department of Health and Human Services: Washington, DC, USA, 2007; p. 582.

28. Wuana, R.A.; Okieimen, F.E. Heavy Metals in Contaminated Soils: A Review of Sources, Chemistry, Risks and Best Available Strategies for Remediation. *ISRN Ecol.* **2011**, *2011*, 402647. [CrossRef]

29. Vodyanitskii, Y.N. Standards for the contents of heavy metals in soils of some states. *Ann. Agrar. Sci.* **2016**, *14*, 257–263. [CrossRef]

30. Tóth, G.; Hermann, T.; Szatmári, G.; Pásztor, L. Maps of heavy metals in the soils of the European Union and proposed priority areas for detailed assessment. *Sci. Total Environ.* **2016**, *565*, 1054–1062. [CrossRef] [PubMed]

31. Tóth, G.; Hermann, T.; Da Silva, M.R.; Montanarella, L. Heavy metals in agricultural soils of the European Union with implications for food safety. *Environ. Int.* **2016**, *88*, 299–309. [CrossRef] [PubMed]

32. Gloag, D. Sources of lead pollution. *Br. Med. J. Clin. Res. Ed.* **1981**, *282*, 41–44. [CrossRef] [PubMed]

33. Bashir, S.; Hussain, Q.; Akmal, M.; Riaz, M.; Hu, H.; Ijaz, S.S.; Iqbal, M.; Abro, S.; Mehmood, S.; Ahmad, M. Sugarcane bagasse-derived biochar reduces the cadmium and chromium bioavailability to mash bean and enhances the microbial activity in contaminated soil. *J. Soils Sediments* **2018**, *18*, 874–886. [CrossRef]

34. Park, J.H.; Lamb, D.; Paneerselvam, P.; Choppala, G.; Bolan, N.; Chung, J.W. Role of organic amendments on enhanced bioremediation of heavy metal(loid) contaminated soils. *J. Hazard. Mater.* **2011**, *185*, 549–574. [CrossRef] [PubMed]

35. Lu, K.; Yang, X.; Shen, J.; Robinson, B.; Huang, H.; Liu, D.; Bolan, N.; Pei, J.; Wang, H. Effect of bamboo and rice straw biochars on the bioavailability of Cd, Cu, Pb and Zn to Sedum plumbizincicola. *Agric. Ecosyst. Environ.* **2014**, *191*, 124–132. [CrossRef]

36. Bian, R.; Joseph, S.; Cui, L.; Pan, G.; Li, L.; Liu, X.; Zhang, A.; Rutlidge, H.; Wong, S.; Chia, C.; et al. A three-year experiment confirms continuous immobilization of cadmium and lead in contaminated paddy field with biochar amendment. *J. Hazard. Mater.* **2014**, *272*, 121–128. [CrossRef] [PubMed]

37. Kan, T.; Strezov, V.; Evans, T.J. Lignocellulosic biomass pyrolysis: A review of product properties and effects of pyrolysis parameters. *Renew. Sustain. Energy Rev.* **2016**, *57*, 126–1140. [CrossRef]

38. Li, J.; Dai, J.; Liu, G.; Zhang, H.; Gao, Z.; Fu, J.; He, Y.; Huang, Y. Biochar from microwave pyrolysis of biomass: A review. *Biomass Bioenergy* **2016**, *94*, 228–244. [CrossRef]

39. Glaser, B.; Lehmann, J.; Zech, W. Ameliorating physical and chemical properties of highly weathered soils in the tropics with charcoal—A review. *Biol. Fertil. Soils* **2002**, *35*, 219–230. [CrossRef]

40. Ahmad, M.; Soo Lee, S.; Yang, J.E.; Ro, H.M.; Han Lee, Y.; Sik Ok, Y. Effects of soil dilution and amendments (mussel shell, cow bone, and biochar) on Pb availability and phytotoxicity in military shooting range soil. *Ecotoxicol. Environ. Saf.* **2012**, *79*, 225–231. [CrossRef] [PubMed]

41. Zhang, R.-H.; Li, Z.-G.; Liu, X.-D.; Wang, B.-C.; Zhou, G.-L.; Huang, X.-X.; Lin, C.-F.; Wang, A.-H.; Brooks, M. Immobilization and bioavailability of heavy metals in greenhouse soils amended with rice straw-derived biochar. *Ecol. Eng.* **2017**, *98*, 183–188. [CrossRef]

42. Mohan, D.; Sarswat, A.; Ok, Y.S.; Pittman, C.U. Organic and inorganic contaminants removal from water with biochar, a renewable, low cost and sustainable adsorbent—A critical review. *Bioresour. Technol.* **2014**, *160*, 191–202. [CrossRef] [PubMed]

43. Tan, X.; Liu, Y.; Zeng, G.; Wang, X.; Hu, X.; Gu, Y.; Yang, Z. Application of biochar for the removal of pollutants from aqueous solutions. *Chemosphere* **2015**, *125*, 70–85. [CrossRef] [PubMed]

44. Kołodyńska, D.; Krukowska, J.; Thomas, P. Comparison of sorption and desorption studies of heavy metal ions from biochar and commercial active carbon. *Chem. Eng. J.* **2017**, *307*, 353–363. [CrossRef]

45. Li, H.; Dong, X.; da Silva, E.B.; de Oliveira, L.M.; Chen, Y.; Ma, L.Q. Mechanisms of metal sorption by biochars: Biochar characteristics and modifications. *Chemosphere* **2017**, *178*, 466–478. [CrossRef] [PubMed]

46. Oliveira, F.R.; Patel, A.K.; Jaisi, D.P.; Adhikari, S.; Lu, H.; Khanal, S.K. Environmental application of biochar: Current status and perspectives. *Bioresour. Technol.* **2017**, *246*, 110–122. [CrossRef] [PubMed]

47. Zhang, C.; Liu, L.; Zhao, M.; Rong, H.; Xu, Y. The environmental characteristics and applications of biochar. *Environ. Sci. Pollut. Res.* **2018**, 21525–21534. [CrossRef] [PubMed]

48. Kasozi, G.N.; Zimmerman, A.R.; Nkedi-Kizza, P.; Gao, B. Catechol and Humic Acid Sorption onto a Range of Laboratory Produced Black Carbons (Biochars). *Environ. Sci. Technol.* **2010**, *44*, 6189–6195. [CrossRef] [PubMed]

49. Mukherjee, A.; Zimmerman, A.R.; Harris, W. Surface chemistry variations among a series of laboratory-produced biochars. *Geoderma* **2011**, *163*, 247–255. [CrossRef]

50. APAT; IRSA/CNR. *Metodi analitici per le acque*; Belli, M., Centioli, D., De Zorzi, P., Sansone, U., Capri, S., Pagnotta, R., Pettine, M., Eds.; APAT: Rome, Italy, 2003; ISBN 88-448-0083-7.

51. Allaire, S.E.; Lange, S.F.; Auclair, I.K.; Quinche, M.; Greffard, L. *Analyses of Biochar Properties*; Centre de Recherche sur les Matériaux Renouvelables, Université Lavall: Québec, QC, Canada, 2015.

52. Pituello, C.; Francioso, O.; Simonetti, G.; Pisi, A.; Torreggiani, A.; Berti, A.; Morari, F. Characterization of chemical–physical, structural and morphological properties of biochars from biowastes produced at different temperatures. *J. Soils Sediments* **2015**, *15*, 792–804. [CrossRef]

53. Qambrani, N.A.; Rahman, M.M.; Won, S.; Shim, S.; Ra, C. Biochar properties and eco-friendly applications for climate change mitigation, waste management, and wastewater treatment: A review. *Renew. Sustain. Energy Rev.* **2017**, *79*, 255–273. [CrossRef]

54. Foo, K.Y.; Hameed, B.H. Insights into the modeling of adsorption isotherm systems. *Chem. Eng. J.* **2010**, *156*, 2–10. [CrossRef]

55. Agarwal, A.K.; Kadu, M.S.; Pandhurnekar, C.P.; Muthreja, I.L. Langmuir, Freundlich and BET Adsorption Isotherm Studies for Zinc ions onto coal fly ash. *Int. J. Appl. Innov. Eng. Manag.* **2014**, *3*, 64–71.

56. Fan, S.; Tang, J.; Wang, Y.; Li, H.; Zhang, H.; Tang, J.; Wang, Z.; Li, X. Biochar prepared from co-pyrolysis of municipal sewage sludge and tea waste for the adsorption of methylene blue from aqueous solutions: Kinetics, isotherm, thermodynamic and mechanism. *J. Mol. Liq.* **2016**, *220*, 432–441. [CrossRef]

57. Ho, Y.S.; McKay, G. Pseudo-second order model for sorption processes. *Process Biochem.* **1999**, *34*, 451–465. [CrossRef]

58. Boni, M.R.; Chiavola, A.; Antonucci, A.; Di Mattia, E.; Marzeddu, S. A novel treatment for Cd-contaminated solution through adsorption on beech charcoal: The effect of bioactivation. *Desalin. Water Treat.* **2018**, *127*, 104–110. [CrossRef]

59. Perry, R.H.; Green, D.W.; Maloney, J.O. *Chemical Engineers' Handbook Seventh*; McGraw-Hill: New York, NY, USA, 1997; Volume 27, ISBN 0070498415.

60. Perry, R.H.; Green, D.W. *Perry's Chemical Engineers' Handbook*; McGraw-Hill: New York, NY, USA, 2008; ISBN 9780071422949.

61. Yoon, Y.H.; Nelson, J.H. Application of Gas Adsorption Kinetics I. A Theoretical Model for Respirator Cartridge Service Life. *Am. Ind. Hyg. Assoc. J.* **1984**, *45*, 509–516. [CrossRef] [PubMed]

62. Thomas, H.C. Heterogeneous Ion Exchange in a Flowing System. *J. Am. Chem. Soc.* **1944**, *66*, 1664–1666. [CrossRef]

63. Bohart, G.S.; Adams, E.Q. Some aspects of the behavior of charcoal with respect to chlorine. *J. Am. Chem. Soc.* **1920**, *42*, 523–544. [CrossRef]

64. Bhaumik, M.; Setshedi, K.; Maity, A.; Onyango, M.S. Chromium(VI) removal from water using fixed bed column of polypyrrole/Fe3O4 nanocomposite. *Sep. Purif. Technol.* **2013**, *110*, 11–19. [CrossRef]

65. Ahmed, M.B.; Zhou, J.L.; Ngo, H.H.; Guo, W.; Chen, M. Progress in the preparation and application of modified biochar for improved contaminant removal from water and wastewater. *Bioresour. Technol.* **2016**, *214*, 836–851. [CrossRef] [PubMed]

66. Noh, J.S.; Schwarz, J.A. Effect of HNO3 treatment on the surface acidity of activated carbons. *Carbon N. Y.* **1990**, *28*, 675–682. [CrossRef]

67. Tag, A.T.; Duman, G.; Ucar, S.; Yanik, J. Effects of feedstock type and pyrolysis temperature on potential applications of biochar. *J. Anal. Appl. Pyrolysis* **2016**, *120*, 200–206. [CrossRef]

68. Kołodyńska, D.; Wnetrzak, R.; Leahy, J.J.; Hayes, M.H.B.; Kwapiński, W.; Hubicki, Z. Kinetic and adsorptive characterization of biochar in metal ions removal. *Chem. Eng. J.* **2012**, *197*, 295–305. [CrossRef]

69. Karunanayake, A.G.; Todd, O.A.; Crowley, M.; Ricchetti, L.; Pittman, C.U.; Anderson, R.; Mohan, D.; Mlsna, T. Lead and cadmium remediation using magnetized and non magnetized biochar from Douglas fir. *Chem. Eng. J.* **2018**, *331*, 480–491. [CrossRef]

70. Rouquerol, J.; Llewellyn, P.; Rouquerol, F. Is the bet equation applicable to microporous adsorbents? *Stud. Surf. Sci. Catal.* **2007**, *160*, 49–56. [CrossRef]

71. Inyang, M.; Gao, B.; Ding, W.; Pullammanappallil, P.; Zimmerman, A.R.; Cao, X. Enhanced lead sorption by biochar derived from anaerobically digested sugarcane bagasse. *Sep. Sci. Technol.* **2011**, *46*, 1950–1956. [CrossRef]

72. Uchimiya, M.; Lima, I.M.; Thomas Klasson, K.; Chang, S.; Wartelle, L.H.; Rodgers, J.E. Immobilization of heavy metal ions (CuII, CdII, NiII, and PbII) by broiler litter-derived biochars in water and soil. *J. Agric. Food Chem.* **2010**, *58*, 5538–5544. [CrossRef] [PubMed]

73. Mohan, D.; Pittman, C.U.; Bricka, M.; Smith, F.; Yancey, B.; Mohammad, J.; Steele, P.H.; Alexandre-Franco, M.F.; Gómez-Serrano, V.; Gong, H. Sorption of arsenic, cadmium, and lead by chars produced from fast pyrolysis of wood and bark during bio-oil production. *J. Colloid Interface Sci.* **2007**, *310*, 57–73. [CrossRef] [PubMed]

74. Harris, W. Dairy-Manure Derived Biochar Effectively Sorbs Lead and Atrazine. *Environ. Sci. Technol.* **2009**, *1*, 3285–3291. [CrossRef]

75. Liu, Z.; Zhang, F.S. Removal of lead from water using biochars prepared from hydrothermal liquefaction of biomass. *J. Hazard. Mater.* **2009**, *167*, 933–939. [CrossRef] [PubMed]

76. Li, Y.-H.; Ding, J.; Luan, Z.; Di, Z.; Zhu, Y.; Xu, C.; Wu, D.; Wei, B. Competitive adsorption of Pb2+, Cu2+ and Cd2+ ions from aqueous solutions by multiwalled carbon nanotubes. *Carbon N. Y.* **2003**, *41*, 2787–2792. [CrossRef]

77. Xue, Y.; Gao, B.; Yao, Y.; Inyang, M.; Zhang, M.; Zimmerman, A.R.; Ro, K.S. Hydrogen peroxide modification enhances the ability of biochar (hydrochar) produced from hydrothermal carbonization of peanut hull to remove aqueous heavy metals: Batch and column tests. *Chem. Eng. J.* **2012**, *200–202*, 673–680. [CrossRef]